ISSN: 3033-358X

Research Article

Journal of Orthopedics and Physiotherapy

Evaluation of Gold Nanoparticles as an Immuno Nutrient

Santhosh Kumar TN* **and Hemalatha MS**

Department of Food Science and Nutrition Karnataka State Open University Mysuru, India

***Corresponding author**
Santhosh Kumar TN, Department of Food Science and Nutrition Karnataka State Open University Mysuru, India.

Received: July 02, 2025; **Accepted:** July 08, 2025; **Published:** July 15, 2025

ABSTRACT

Introduction: The Gold nanoparticles obtained from different nano particles production company namely Shree Dhootpapeshwar Limited and Nanoshel company based in United Kingdom are of their unique properties. In this study we are going to analyze the invitro properties of these gold nanoparticles for their hypothesized properties of immune nutrition.

Objectives: To study the immune modulation properties of gold nanoparticles. To analyze the nutritional composition of gold nanoparticles.

Methodology: The Fourier Transform Infrared Spectrometry was used for the analysis of gold nanoparticles from two sources in the Centre for Nano Science and Engineering (CeNSE), Indian Institution of Science, Bengaluru.

Results: The Gold nanoparticles I (AuNPs-I) and gold nanoparticles II(AuNPs-II) showed wavelength of 3435.67/cm and 3435.98/cm respectively.

Discussion and Conclusion: FTIR- Fourier Transform Infrared spectrophotometer works in the mid- infrared light to measure the light absorption in 400-4000/cm 92.5-25micrometer to identify and measure the quantity of different materials. The comparative FTIR analysis demonstrated clear differences in the surface functional groups of two gold nanoparticle samples synthesized by different methods. These differences underscore the importance of synthesis conditions in determining the surface chemistry and potential functionality of AuNPs. Such insights are essential for guiding the design of nanoparticles for targeted applications in fields such as biomedicine, catalysis, and sensing.

Keywords: Gold Nanoparticles (AuNPs), Fourier Transform Infrared spectrophotometer (FTIR), Surface Chemistry

Introduction

Gold nanoparticles (AuNPs) have gained significant attention due to their unique optical, electronic, and chemical properties. These characteristics are highly influenced by surface modifications, which are in turn determined by the synthesis method and capping agents used. FTIR spectroscopy is a powerful technique for analyzing the surface chemistry of nanoparticles, providing insights into the nature of the functional groups present. This study aims to compare the FTIR spectra of two differently synthesized AuNP samples to evaluate their surface functionalities and potential implications for their application.

Antimicrobial resistance (AMR) is currently one of the biggest threats to global health and food security, according to the World Health Organization (WHO) [1]. A study from data reported by 87 countries in 2020 revealed high AMR levels, which cause potentially fatal sepsis, as well as growing resistance to treatment in various bacteria that cause common infections among the population [2]. Therefore, there is an urgent need to find new, more effective antibiotics to counteract these resistances. However, clinical development of new antimicrobials is very

Citation: Santhosh Kumar TN, Hemalatha MS. Evaluation of Gold Nanoparticles as an Immuno Nutrient. J Ortho Physio. 2025. 3(3): 1-8.
DOI: doi.org/10.61440/JOP.2025.v3.29

limited. In 2019, thirty-two antibiotics were in the development phase, and only six were classified as innovators [3]. This problem affects countries at all levels of development. Due to the complexity and breadth of the AMR problem, a unified multisectoral view is required, using the "one health" approach, to establish communication ties and collaborate in the project and implementation of programs, policies, legislation, and research to achieve better public health outcomes [4]. Understanding of the different mechanisms of antimicrobial resistance is very impor tant for th creation of new alternatives to counteract it. Some examples of these resistance mechanisms are avoiding the accumulation of antibiotics, the modification of the target molecules, and the enzymatic inactivation of antibiotics. The first type of mechanism can reduce the absorption of these molecules by modifying the outer bacterial membrane (losing or modifying the porins to prevent antibiotic access), increasing their discharge through the pumps, or both. Hydrophobic antibiotics, such as quinolones and macrolides, pass through the lipid bilayer, whereas hydrophilic antibiotics, such as beta-lactams, pass through porins [5,6]. This may be an innate characteristic of an organism or may be produced by a mutation or acquisition of exogenous resistance genes [7]. One antibiotic that covers a broad spectrum of antimicrobial activity is amoxicillin (AMOX), whose use dates from the 1970s. This semisynthetic penicillin is the most widely used in the world, either alone or combined with clavulanic acid [8]. According to the American Society of Health-System Pharmacists, AMOX prevents bacterial growth. It is used in the treatment of bacterial infections such as pneumonia and bronchitis, and ear, nose, throat, urinary tract, and skin infections. AMOX binds to penicillin-binding protein (PBP) 1A, an enzyme that is essential for the synthesis of the bacterial cell wall. The-lactam ring of amoxicillin modifies the carbon terminus of the PBP 1A transpeptidase. It forms an irreversible union that prevents the enzyme from carrying out its function of synthesizing peptidoglycan, which makes up the bacterial wall. This will ultimately result in an alteration of the membrane and an increase in its permeability, leading to cell lysis and death [8]. AMOX has a hydroxyl group that makes it more soluble in lipids, and therefore gives it greater bioavailability, duration of action, and bactericidal activity. AMOX is normally administered orally, and it is usually rapidly absorbed, presenting greater bioavailability. Adverse effects must also be considered. In this sense, AMOX presents some toxicity, sometimes causing lesions in the bile ducts, as well as hypersensitivity reactions [9,10]. The resistant bacteria used in this work are Escherichia coli (E. coli), Streptococcus pneumoniae (S. pneumoniae) and Staphylococcus aureus (S. aureus). E. coli is a Gram-negative bacterium that is classified as a member of the Enterobacteriaceae family. E. coli includes not only commensal but also pathogenic strains that cause a variety of human diseases, resulting in millions of deaths each year due to virulence factors and pathogenicity mechanisms that cause gastrointestinal diseases like diarrhea ; other strains can cause haemolytic uraemic syndrome and hemorrhagic colitis, leading to acute renal failure, which can cause death. E [11]. coli also has a large environmental impact on water quality and public health [12]. S. aureus, a Gram-positive microorganism, can survive in very adverse conditions, easily colonizing the skin and therefore penetrating tissues. The most frequent pathologies of S. aureus are infections of the skin and soft tissues, otitis, osteomyelitis, arthritis, pneumonia, and sepsis, generating the majority of nosocomial diseases [13]. S. pneumoniae is a Gram-positive bacterial pathogen that may asymptomatically colonize the upper respiratory tract and can cause infections including conjunctivitis, otitis media, lower respiratory tract infections, bacteremia, and meningitis [14,15]. The mechanisms of antibiotic resistance of S. pneumoniae include the evolution of resistance patterns and mechanisms for beta-lactam antibiotics, among others [16,17]. Knowledge of the different mechanisms of resistance to antimicrobials is essential to be able to propose new strategies that solve the problem of resistance to antibiotics. Among the different mechanisms studied are those based on the production of enzymes that are inactivating; there are also those based on modifications of the therapeutic target, and others that act by decreasing the intracellular concentration of the antibiotic [18]. The mechanisms of intracellular antibiotic reduction may be due to a mechanism based on efflux pumps that expel the antibiotic, or a mechanism that modifies the external bacterial membrane, so that the bacteria lose or modify porins, thereby preventing the entry of the antibiotic [19]. An example of these are beta-lactams, hydrophilic antibiotics that cross porins, or the use of vehicles made up of gold nanoparticles (AuNPs) that can interact with the exterior of the microorganism, destabilizing its exterior [20,21].

Nanoparticles have numerous biological, biomedical, pharmaceutical, and nutritional applications [22]. Materials at the nanoscale (1–100 nm) display unique physicochemical properties, and their small size allows them to penetrate bacterial membranes (>1 m). Some studies also show that metal nanoparticles have antimicrobial activity in themselves, especially metal nanoparticles, with the advantage that microorganisms are not able to create resistance to such materials. Nano systems are based on the idea of the Trojan horse, and have been highly successful in the pharmaceutical industry because they exhibit stable drug loading, expanded pharmacokinetics, reduced off-target side effects, and improved efficiency of drug delivery through their ability to penetrate blood–brain barriers or plasma membranes [23,24]. In recent years, there has been increasing interest in the development of optimal metal-base nanoparticles (MBNPs) and their usage synergy with antibiotics for combating antibiotic-resistant bacteria [25]. In this context, MBNPs–antibiotic/biopolymer biomaterials have been demonstrated to be crucial due for the potential synergistic functionalities of these kinds of complexes, which are different from those presented in their individual counterparts. Forming part of these nanocomplexes, distinct oxides like TiO, ZnO, and the nanometallic Ag, among others, are specifically found in the bibliography [26-33]. Metallic nanomaterials affect the bacterial cell membrane, and they can release antibacterial metal ions, generate reactive oxygen species, inhibit enzymatic activity and DNA synthesis, and interrupt energy transmission [34]. However, the principal mechanism of action of MBNPs includes the production of oxidative stress, interaction with cell membrane, or the release of ions [25]. This occurs n such a way that these new nanomaterials not only improve the sustained release of the antibiotic, but also enhance the antibacterial effect of the drug in comparison with the conventional usage of the free antibiotic. For instance, Ag-based nano systems can act through multiple mechanisms, depending on the specific nano formulation. Thus, they can act by generating oxidative stress, interacting with

the cellular membrane without damaging the outer membrane, thereby contributing to the release of ions and preventing DNA replication, or acting as enzyme inhibitors, such is the diversity of the mechanisms studied to date. In contrast, the mechanism of action of Au-based nano systems has been less explored, and the majority of the studies in the bibliography indicate that the mechanism of the cations of this kind of metal nanoparticle is fundamentally based on oxidative stress oxidation [31-35]. However, AuNPs offer certain advantages over other metallic nanoparticles. As is known, AuNPs improve nano system biocompatibility and protect against enzymatic degradation exerted on biomolecules like DNA or ribonucleic acid (RNA) [36]. Thus, the combined use of AuNPs and the DNA biopolymer contributes to overcoming problems related to biocompatibility. Moreover, the small size of the synthesized nano formulations makes them capable of diffusing effectively through the bacterial cell wall, thus improving internalization and interaction with the bacteria, as has been demonstrated in previous works [37,38]. Therefore, the main objective of this work is to obtain stable and biocompatible AuNPs for evaluating their synergistic antibacterial effects caused by both the precursors. 16-mph-16 is a biocompatible and biodegradable Gemini surfactant with a benzene spacer that shows great antibacterial properties against distinct bacteria and microscopic fungi. For instance, the MIC values of the analogous 16-Ph-16 against E. coli and S. aureus bacteria were found to be 0.3906 and 1.5625 mM, respectively [39]. Moreover, this type of surfactant has proven to be very efficient in DNA compaction, inter acting strongly with DNA via partial intercalation [40]. Thus, the combination of both the antimicrobial properties of 16-mph-16-covered AuNPs and a DNA-AMOX complex in a unique nano system result in a nano formulation that acts quickly, favoring microbial death with a small amount of antibiotic, thereby combating resistance to antibiotics in addition to avoiding the secondary side effects derived from the administration of high doses of antibiotics.

Objectives

To study the immune modulation properties of gold nanoparticles.
To analyze the nutritional composition of gold nanoparticles.

Methodology

The Fourier Transform Infrared Spectrometry was used for the analysis of gold nanoparticles from two sources in the Centre for Nano Science and Engineering (CeNSE), Indian Institution of Science, Bengaluru.

Two samples of AuNPs, labeled AuNPs_1_1 and AuNPs_2_1, were obtained from the pharmacy. The nanoparticles were washed and dried before FTIR analysis. FTIR spectra were recorded in the range of 4000 to 400 cm\u207b\u00b9 using a standard ATR-FTIR spectrometer. Spectral data were processed and analyzed to identify key vibrational bands.

Results and Discussion

The FTIR analysis confirms the successful functionalization of AuNPs with biomolecules, as evident from the presence of hydroxyl, carbonyl, and amide functional groups. These functional moieties play a crucial role in the reduction of Au^{3+} to Au^{0} and the stabilization of nanoparticles in colloidal form.

FTIR Interpretation and Discussion

FTIR spectroscopy was employed to analyze the surface chemistry and functional groups involved in the reduction and stabilization of synthesized gold nanoparticles (AuNPs). The FTIR spectra of both samples revealed several characteristic absorption bands corresponding to organic functional groups, suggesting the presence of bioactive molecules acting as capping and stabilizing agents.

Key Peaks and Assignments:

- ~3400–3200 cm^{-1} (broad): A prominent peak in this region corresponds to O–H stretching vibrations of hydroxyl groups, commonly present in polyphenols, alcohols, or water molecules associated with biomolecules. It may also indicate N–H stretching from amines or proteins, suggesting the involvement of natural reducing agents.
- ~2920–2850 cm^{-1}: These peaks are typically attributed to the C–H stretching vibrations of aliphatic $–CH_2$ and $–CH_3$ groups, indicating the presence of long-chain hydrocarbons or lipids on the nanoparticle surface.
- ~1650 cm^{-1}: A sharp peak here indicates C=O (carbonyl) stretching vibrations, which may originate from amide I bands of proteins or other carbonyl-containing compounds. This confirms the interaction of carbonyl-rich biomolecules in the reduction or capping process.
- ~1540 cm^{-1}: This band corresponds to N–H bending (amide II band), commonly found in proteins or amino compounds, suggesting the stabilization of nanoparticles via protein adsorption.
- ~1400–1380 cm^{-1}: The observed peak in this region is associated with C–N stretching or symmetric bending of CH_3 groups, supporting the presence of amino acid residues or other organic moieties.
- ~1050–1000 cm^{-1}: This peak represents C–O stretching vibrations found in alcohols, ethers, or polysaccharides, indicating that carbohydrate components or flavonoids may be involved in capping the AuNPs. (Figure 1)

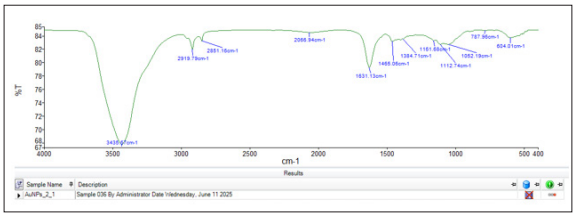

Figure 1: FTRI Analysis of Sample AuNPs_2_1

FTIR Spectrum Interpretation – AuNPs_2_1

The FTIR spectrum of the synthesized gold nanoparticles (AuNPs_2_1) exhibits distinct peaks that indicate the presence of various functional groups, suggesting successful surface modification or capping of the AuNPs:

- The broad peak at 3435.97 cm^{-1} corresponds to O–H stretching, indicating the presence of hydroxyl groups, likely from polyols, alcohols, or water molecules associated with the capping/stabilizing agent.
- Peaks at 2919.79 and 2851.16 cm^{-1} suggest C–H stretching vibrations, indicative of aliphatic chains commonly found in organic stabilizers such as citrate, PEG, or plant-derived extracts.

- The peak at 1631.13 cm^{-1} could arise from C=O (amide I) or C=C (aromatic) stretching, implying the presence of proteins or phenolic compounds, especially if biosynthesis was employed.
- The region between 1465 and 1052 cm^{-1} includes various bending and stretching modes for CH_2, C–N, and C–O, further supporting the presence of organic molecules involved in nanoparticle stabilization.
- The sharp peaks at lower wavenumbers (787.96 and 604.01 cm^{-1}) may correspond to aromatic C–H bending and metal–ligand interactions, particularly Au–O or Au–N bonds, confirming the binding of organic molecules to the gold nanoparticle surface. (Table 1)

Table 1: FTRI Analysis of Sample AuNPs_2_1

Peak Position (cm^{-1})	Possible Functional Group/Assignment
3435.97	O–H stretching (broad) – likely alcohol or phenol groups (possibly from capping agents or water)
2919.79	C–H stretching – aliphatic hydrocarbons
2851.16	C–H symmetric stretching – CH_2/CH_3 groups
2065.94	Possibly –C≡C– or –N=C=S stretch (rare, may be artifact or reagent trace)
1631.13	C=C or C=O stretching – typical of aromatic rings or amide carbonyls
1465.06	CH_2 bending or scissoring – alkanes or alkyl chains
1384.71	C–H bending – methyl groups
1161.68	C–O–C or C–N stretching – esters or amines (stabilizers)
1112.74	C–O stretching – ethers or alcohol groups
1052.19	C–O stretching – primary alcohols or esters
787.96	Aromatic C–H bending – possibly phenyl ring substitution
604.01	Metal–O or Au–O stretching – indicates gold-ligand interaction

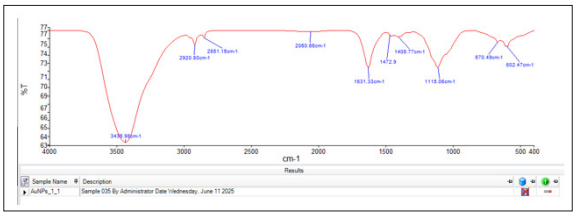

Figure 2: FTRI Analysis of Sample AuNPs_1_1

The FTIR analysis of the synthesized gold nanoparticles (AuNPs_1_1) provides significant insight into the functional groups involved in the reduction and stabilization processes. The broad absorption peak at **3435.98 cm^{-1}** is attributed to O–H stretching vibrations, indicating the presence of hydroxyl groups. This suggests the involvement of polyphenols or other hydroxyl-containing compounds, likely originating from plant extracts or water molecules adsorbed on the nanoparticle surface.

Table 2: FTRI analysis of sample AuNPs_2_1

Wavenumber (cm^{-1})	Possible Functional Group / Vibration	Interpretation
3435.98	O–H stretching (broad)	Presence of hydroxyl groups; possibly from alcohols or phenols, or water molecules adsorbed on the surface.
2920.80 & 2851.15	C–H stretching (alkanes)	Indicates –CH_2 or –CH_3 groups from capping agents like citrate or plant extracts.
2060.66	–N=C=S or other isocyanide type stretching	May suggest the presence of certain functional groups from stabilizers or organic molecules.
1631.33	C=O stretching (amide I or conjugated ketones)	Possible amide group (from proteins or capping agents like peptides) or C=C stretching.
1472.9 & 1405.77	C–H bending / COO^- symmetric stretching	Presence of carboxylate groups –COO^-, indicating citrate or other capping agents.
1115.06	C–O stretching (alcohols, ethers)	Suggests polysaccharides or other stabilizers.
670.49 & 602.47	Metal–oxygen or out-of-plane bending	May indicate metal–ligand interactions or Au–O type bonds.

The peaks observed at **2920.80 cm^{-1}** and **2851.15 cm^{-1}** correspond to asymmetric and symmetric C–H stretching vibrations of methylene (–CH_2) groups, which are characteristic of aliphatic chains. These signals imply the presence of organic stabilizing agents, possibly from capping materials like citrate ions or plant-derived compounds.

A weak absorption band at **2060.66 cm^{-1}** may be assigned to isocyanide or related functional groups, indicating the presence of trace organic residues involved in nanoparticle stabilization or formation.

A prominent peak at **1631.33 cm^{-1}** is associated with C=O stretching vibrations, suggesting the presence of amide or conjugated carbonyl groups. This could indicate the involvement of proteinaceous molecules or other biomolecules in the capping process. The adjacent bands at **1472.9 cm^{-1}** and **1405.77 cm^{-1}** are likely due to C–H bending and symmetric stretching of carboxylate (–COO^-) groups, further supporting the presence of citrate or similar carboxyl-containing capping agents.

The strong absorption at **1115.06 cm⁻¹** is assigned to C–O stretching vibrations, indicative of alcohols or ethers, possibly from polysaccharides or plant-derived biomolecules used during the synthesis. Peaks at lower wavenumbers, such as **670.49 cm⁻¹** and **602.47 cm⁻¹**, may correspond to metal–oxygen interactions or Au–O vibrations, suggesting successful binding of functional groups to the gold nanoparticle surface. (Figure 2) (Table 2).

Overall, the FTIR spectrum confirms the successful reduction and stabilization of gold nanoparticles using biologically derived compounds. The presence of hydroxyl, carboxyl, and carbonyl functional groups suggests that phytochemicals or other biomolecules not only facilitated the reduction of Au^{3+} ions to Au^0 but also acted as efficient capping agents, enhancing the stability of the synthesized nanoparticles.

- The FTIR spectrum confirms the presence of functional groups associated with capping and stabilizing agents used in the synthesis of gold nanoparticles.
- Strong O–H, C=O, and C–O peaks point to organic biomolecules or plant extract residues.
- The C–H and COO^- peaks suggest stabilizers like citrate or natural reducing agents were involved.

Low wavenumber peaks (~600 cm^{-1}) may be attributed to Au–O interactions or metal–ligand bonding, suggesting successful nanoparticle formation and stabilization.

Fourier-transform infrared spectroscopy (FTIR) was employed to analyze the functional groups present on the surface of two synthesized gold nanoparticle (AuNP) samples, **AuNPs_1_1** and **AuNPs_2_1**. The FTIR spectra of both samples (Figures 1 and 2) revealed multiple characteristic absorption bands corresponding to various organic functional groups, indicating successful surface modification or capping of the nanoparticles.

FTIR Spectral Analysis

Both samples exhibited a broad absorption peak around 3435 cm^{-1}, attributed to O–H stretching vibrations. This indicates the presence of hydroxyl groups, possibly from water, alcohols, or phenolic compounds used as stabilizing agents.

Peaks in the region of 2919–2851 cm^{-1}, observed in both spectra, correspond to C–H stretching vibrations of aliphatic $–CH_2$ and $–CH_3$ groups. These are indicative of the presence of long-chain organic molecules, such as those found in surfactants, reducing agents (e.g., plant extracts), or capping agents (e.g., citrate or polyethylene glycol).

Both samples also displayed a strong peak around **1631 cm⁻¹**, attributed to either C=C stretching in aromatic rings or C=O stretching in amide groups (amide I band), suggesting the involvement of organic ligands such as proteins or polyphenolic compounds in the stabilization of AuNPs.

Notably, **AuNPs_2_1** displayed **additional peaks at 1384.71, 1161.68, 1112.74, 1052.19, and 787.96 cm⁻¹**, which were either absent or less prominent in **AuNPs_1_1**. These peaks indicate the presence of **C–N stretching (amines), C–O stretching (ethers or esters), and aromatic ring vibrations**, suggesting a more complex capping composition in **AuNPs_2_1**. The presence of these functional groups may imply improved stability or functional versatility.

Conversely, **AuNPs_1_1** showed fewer distinct peaks in the fingerprint region (1500–500 cm^{-1}), with only moderate signals at **1405.77, 1115.06, 670.49, and 602.47 cm⁻¹**, reflecting a comparatively **simpler surface chemistry. (Figure 3)**

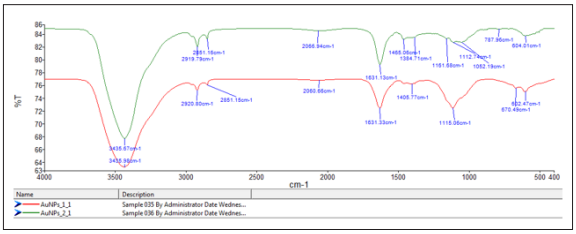

Figure 3: FTIR Spectral Analysis of Both Samples

Table 3: FTIR Spectral Analysis of Both Samples.

Functional Group Region	AuNPs_1_1	AuNPs_2_1	Interpretation
O–H Stretch (3435 cm^{-1})	Present	Present	Surface hydroxyls or absorbed moisture
C–H Stretch (2919–2851)	Present	Present	Aliphatic chains (capping agents)
C=O / C=C Stretch (1631)	Present	Present	Amide I / aromatic ring
C–O / C–N (1100–1300)	Moderate	Strong, multiple peaks	Rich organic matrix in AuNPs_2_1
Au–O / Aromatic bends	670–602 cm^{-1}	787–604 cm^{-1}	Slight differences in metal–ligand interactions

FTIR (Fourier Transform Infrared Spectroscopy) comparison graph of two gold nanoparticle (AuNP) samples: **AuNPs_1_1** (green) and **AuNPs_2_1** (red). The x-axis represents wavenumbers (cm^{-1}), which correspond to the frequency of infrared light absorbed, and the y-axis represents % Transmittance (%T), indicating how much light passes through the sample. (Figure 3)

1. Broad Peak Around 3400 cm^{-1}:
- AuNPs_1_1 (green): 3435.67, 3435.98 cm^{-1}
- AuNPs_2_1 (red): Absent
- Interpretation: This broad peak is typically due to O–H stretching (hydroxyl groups), suggesting the presence of alcohols or water in AuNPs_1_1, but not in AuNPs_2_1.

2. Peaks Around 2900 cm^{-1} (C–H stretching):
- Both samples show peaks around 2851–2920 cm^{-1}
- Interpretation: Common for aliphatic C–H bonds, indicating organic stabilizing agents in both samples.

3. Peak at ~2060 cm^{-1}:
- Present in both samples
- Could relate to C≡C (alkyne) or N=C=O (isocyanate) groups.
4. Peaks Around 1631 cm^{-1}:
- Present in both samples.
- Interpretation: C=C stretching or amide I band (in proteins), indicating possible protein or biomolecule capping.
5. Peaks in Fingerprint Region (1400–500 cm^{-1}):
- AuNPs_1_1 shows more distinct peaks (e.g., 1384.71, 1161.68, 1052.19, 787.96 cm^{-1})
- AuNPs_2_1 has peaks like 1115.06, 682.47 cm^{-1}
- Interpretation: These differences suggest variation in surface functionalization or capping agents between the two samples.
- AuNPs_1_1 shows strong hydroxyl group presence, indicating either moisture content or hydroxyl-rich capping agents.
- AuNPs_2_1 lacks this OH stretch but still shows common organic and protein-related functional groups.
- Differences in the fingerprint region suggest distinct surface chemistry, which could result from using different reducing or capping agents in synthesis. (Table 3)

Conclusion

The FTIR spectra of two synthesized gold nanoparticle samples, AuNPs_1_1 and AuNPs_2_1, were analyzed to evaluate the differences in surface functional groups, which indicate variation in synthesis conditions or capping agents used.

A prominent broad peak around **3435 cm^{-1}** was observed exclusively in AuNPs_1_1, corresponding to **O–H stretching vibrations**. This suggests the presence of hydroxyl-containing compounds, such as alcohols or adsorbed water molecules, which may indicate either incomplete drying or the use of a polyhydroxylated capping agent (e.g., plant extract or polyol). In contrast, the absence of this peak in AuNPs_2_1 suggests a relatively lower presence of free hydroxyl groups or more complete drying.

Both spectra displayed **C–H stretching vibrations** in the **2851–2921 cm^{-1}** range, indicating the presence of **aliphatic hydrocarbon** chains. These peaks are typically associated with organic molecules, suggesting that both samples were capped or stabilized with organic agents, possibly surfactants or natural polymers.

A notable absorption near **2060 cm^{-1}** in both spectra may correspond to **N=C=O stretching** (isocyanate groups) or possibly **C≡C stretching** (alkyne groups), although further confirmation is required. Its presence in both samples indicates a common feature or residual reagent used during synthesis.

Both samples also exhibited a peak at **1631 cm^{-1}**, which could be attributed to **C=C stretching** in alkenes or **amide I bands**, indicative of proteinaceous material. This suggests the possible involvement of amino acid or protein-based reducing/stabilizing agents, especially if biosynthetic methods were employed.
Significant variations were observed in the **fingerprint region (1500–500 cm^{-1})**, with AuNPs_1_1 showing more complex and intense peaks (e.g., 1384.71, 1161.68, 1052.19, 787.96 cm^{-1}) compared to AuNPs_2_1 (e.g., 1115.06, 682.47 cm^{-1}). These differences suggest that **different functional groups are bound to the nanoparticle surfaces**, likely due to different synthesis precursors or capping agents.

Overall, the FTIR analysis confirms that both samples are coated with organic molecules but differ in specific surface functionalities. These variations could influence the **colloidal stability, biological compatibility**, and reactivity of the nanoparticles and should be considered when selecting the appropriate synthesis method for targeted applications.

Fourier Transform Infrared Spectroscopy (FTIR) was employed to investigate the surface functional groups present in two synthesized gold nanoparticle samples, designated as AuNPs_1_1 and AuNPs_2_1. The comparative analysis revealed significant differences in the vibrational profiles of the two samples, indicative of variations in the capping agents or synthesis conditions employed.

A broad absorption band centered at **3435 cm^{-1}** was observed prominently in the spectrum of AuNPs_1_1 but was absent in AuNPs_2_1. This band corresponds to the **O–H stretching vibration**, typically associated with hydroxyl groups from alcohols or adsorbed water molecules. The presence of this peak suggests that AuNPs_1_1 may have been synthesized using a polyhydroxylated compound, such as a plant extract or polyol, acting as both reducing and stabilizing agent. The absence of this band in AuNPs_2_1 implies a difference in the surface chemistry, possibly due to the use of less polar or more hydrophobic capping agents.

Both samples exhibited characteristic **C–H stretching vibrations** in the region of **2851–2921 cm^{-1}**, consistent with the presence of aliphatic hydrocarbon chains. These signals are indicative of organic molecules, possibly surfactants, thiols, or polymers, that are bound to the nanoparticle surface and contribute to colloidal stability.

An absorption peak observed at approximately **2060 cm^{-1}** in both spectra may be attributed to isocyanate **(–N=C=O) or alkyne (–C≡C–)** functional groups. While less commonly reported in gold nanoparticle systems, the presence of this band in both samples could indicate a shared synthetic reagent or intermediate compound with these functional moieties.

Notably, both samples exhibited a peak at **1631 cm^{-1}**, assignable to **C=C stretching** in alkenes or possibly to the **amide I band** of proteins, which typically arises from C=O stretching vibrations in peptide bonds. This suggests that proteinaceous or amino acid-containing materials may have been involved in the synthesis process, particularly if biosynthetic or green synthesis approaches were utilized.

The **fingerprint region (1500–500 cm^{-1})** showed clear distinctions between the two samples. AuNPs_1_1 displayed multiple well-defined peaks, including at **1384.71, 1161.68, 1052.19, and 787.96 cm^{-1}**, whereas AuNPs_2_1 exhibited peaks at **1115.06, 682.47, and 570.49 cm^{-1}**. These differences strongly indicate **variation in surface-bound functional groups**, which could arise from different capping agents or reducing agents used during synthesis. Such molecular differences can significantly

affect the nanoparticles' surface reactivity, dispersion behavior, and interaction with biological systems.

In summary, FTIR spectral analysis reveals distinct surface chemical signatures for AuNPs_1_1 and AuNPs_2_1. These findings underscore the impact of synthesis conditions on the chemical composition of the nanoparticle surface, which in turn may influence their functional properties, including stability, biocompatibility, and potential application in biomedical or catalytic systems.

Reference

1. World Health Organization Antibiotic Resistance https://www.who.int/news-room/fact-sheets/detail/.
2. World Health Organization. Global Antimicrobial Resistance and Use Surveillance System (GLASS) Report 2022, World Health Organization: Geneva Switzerland 2022 ISBN 9789240062702.
3. Hutchings M, Truman A, Wilkinson B. Antibiotics: Past, Present and Future. Curr Opin Microbiol. 2019. 51: 72-80.
4. Adisasmito WB, Almuhairi S, Behravesh CB, Bilivogui P, Bukachi SA, et al. One Health: A New Definition for a Sustainable and Healthy Future. PLoS Pathog. 2022. 18: e1010537.
5. Chapman JS, Georgopapdakou NH. Routes of Quinolone Permeation in Escherichia Coli. Antimicrob. Agents Chemother. 1988. 32: 438-442.
6. Delcour AH. Outer Membrane Permeability and Antibiotic Resistance. Biochim Biophys Acta Proteins Proteom. 2009. 1794: 808-816.
7. Poole K. Efflux-Mediated Antimicrobial Resistance. J Antimicrob Chemother. 2005. 56: 20-51.
8. Huttner A, Bielicki J, Clements MN. Frimodt-Møller N. Muller AE, et al. Oral Amoxicillin and Amoxicillin–Clavulanic Acid: Properties, Indications and Usage. Clin Microbiol Infect. 2020. 26: 871-879.
9. Visentin M, Lenggenhager D, Gai Z, Kullak-Ublick GA. Drug-Induced Bile Duct Injury. Biochim Biophys Acta Mol Basis Dis. 2018. 1864: 1498-1506.
10. Dhir A, Kular H, Elzagallaai AA, Carleton B, Rieder MJ, et al. DRESS Induced by Amoxicillin-Clavulanate in Two Pediatric Patients Confirmed by Lymphocyte Toxicity Assay. Allergy Asthma Clin Immunol. 2021. 17: 37.
11. Kaper JB, Nataro JP, Mobley HLT. Pathogenic Escherichia Coli. Nat Rev Microbiol. 2004. 2: 123-140.
12. Jang J, Hur H-G, Sadowsky MJ, Byappanahalli MN, Yan T, et al. Environmental Escherichia Coli: Ecology and Public Health Implications—A Review. J Appl Microbiol. 2017. 123: 570-581.
13. Prieto J, García del Potro M, Gómez-Lus Centelles ML. Guía Para El. Antibiotic Use in Primary Care. In Vivo Efficacy, In Vitro Efficacy; Doyma Editions: Madrid. Spain. 1997. 83-96.
14. Tomasz A. Antibiotic Resistance in Streptococcus Pneumoniae. Clin Infect Dis. 1997. 24: S85–S88.
15. Henriques-Normark B, Tuomanen EI. The Pneumococcus: Epidemiology, Microbiology, and Pathogenesis. Cold Spring Harb. Perspect Med. 2013. 3: a010215.
16. Appelbaum PC. Resistance among Streptococcus Pneumoniae: Implications for Drug Selection. Clin Infect Dis 2002: 34: 1613-1620.
17. Cherazard R, Epstein M, Doan TL, Salim T, Bharti S, et al. Antimicrobial Resistant Streptococcus Pneumoniae: Prevalence, Mechanisms, and Clinical Implications. Am J Ther. 2017. 24: e361-e369.
18. Prats G. Medical Microbiology and Parasitology, 1st ed. Panamericana Medical Publishing Madrid Spain. 2013. 1.
19. Cag Y, Caskurlu H, Fan Y, Cao B, Vahaboglu H. Resistance Mechanisms. Ann Transl Med 2016. 4: 326.
20. Oteo Iglesias J. Antibiotic Resistance: The Threat of Superbugs. Los Libros de la Catarata Madrid Spain. 2016..
21. Giráldez-Pérez RM, Grueso EM, Jiménez-Aguayo R, Carbonero A, González-Bravo M, et al. Use of Nanoparticles to Prevent Resistance to Antibiotics—Synthesis and Characterization of Gold Nanosystems Based on Tetracycline. Pharmaceutics. 2022. 14: 1941.
22. Abdullah SS, Masood S, Zaneb H, Rabbani I, Akbar J, et al. Effects of CopperNanoparticles on Performance, Muscle and Bone Characteristics and Serum Metabolites in Broilers | Efeitos de Nano partículas de Cobre No Desempenho, Características Musculares e Ósseas e Metabólitos Séricos Em Frangos de Corte. Braz J Biol 2024. 84: e261578.
23. Al-Awsi GRL, Alameri AA, Al-Dhalimy AMB, Gabr GA, Kianfar E. Application of Nano-Antibiotics in the Diagnosis and Treatment of Infectious Diseases | Aplicação de Nanoantibióticos No Diagnóstico e Tratamento de Doenças Infecciosas. Braz. J Biol. 2023. 84: e264946.
24. Fan Y, Marioli M, Zhang K. Analytical Characterization of Liposomes and Other Lipid Nanoparticles for Drug Delivery. J Pharm. Biomed Anal. 2021. 192: 113642.
25. Altun E, Aydogdu MO, Chung E, Ren G, Homer-Vanniasinkam S, et al. Metal-Based Nanoparticles for Combating Antibiotic Resistance. Appl Phys Rev. 2021. 8: 041303.
26. Planchon M, Ferrari R, Guyot F, Gélabert A, Menguy N, et al. Interaction between Escherichia Coli and TiO2 Nanoparticles in Natural and Artificial Waters. Colloids Surf. B Biointerfaces. 2013. 102: 158-164.
27. Kiwi J, Nadtochenko V. Evidence for the Mechanism of Photocatalytic Degradation of the Bacterial Wall Membrane at the TiO2 Interface by ATR-FTIR and Laser Kinetic Spectroscopy. Langmuir. 2005. 21: 4631-4641.
28. Singh R, Cheng S, Singh S. Oxidative Stress-Mediated Genotoxic Effect of Zinc Oxide Nanoparticles on Deinococcus Radiodu- rans. 3 Biotech. 2020. 10: 66.
29. Cha SH, Hong J, McGuffie M, Yeom B, Vanepps JS, et al. Shape-Dependent Biomimetic Inhibition of Enzyme by Nanoparticles and Their Antibacterial Activity. ACS Nano. 2015. 9: 9097-9105.
30. Khan ST, Malik A, Wahab R, Abd-Elkader OH, Ahamed M, et al. Synthesis and Characterization of Some Abundant Nanoparticles, Their Antimicrobial and Enzyme Inhibition Activity. Acta Microbiol Immunol Hung. 2017: 64: 203-216.
31. Quinteros MA, Cano Aristizábal V, Dalmasso PR, Paraje MG, Páez PL. Oxidative Stress Generation of Silver Nanoparticles in Three Bacterial Genera and Its Relationship with the Antimicrobial Activity. Toxicol Vitr. 2016. 36: 216-223.
32. Seong M, Lee DG. Silver Nanoparticles Against Salmonella Enterica Serotype Typhimurium: Role of Inner Membrane Dysfunction. Curr Microbiol. 2017. 74: 661-670.

33. Li R, Chen J, Cesario TC, Wang X, Yuan JS, et al. Synergistic Reaction of Silver Nitrate, Silver Nanoparticles, and Methylene Blue against Bacteria. Proc. Natl Acad Sci. 2016. 113: 13612-13617.
34. Zhao X, Tang H, Jiang X. Deploying Gold Nanomaterials in Combating Multi-Drug-Resistant Bacteria. ACS Nano. 2022. 16: 10066-10087.
35. Mohamed MM, Fouad SA, Elshoky HA, Mohammed GM, Salaheldin TA. Antibacterial Effect of Gold Nanoparticles against Corynebacterium Pseudotuberculosis. Int J Vet Sci Med. 2017. 5: 23-29.
36. Ghosh PS, Kim CK, Han G, Forbes NS, Rotello VM. Efficient Gene Delivery Vectors by Tuning the Surface Charge Density of Amino Acid-Functionalized Gold Nanoparticles. ACS Nano. 2008. 2: 2213-2218.
37. Lu Z, Rong K, Li J, Yang H, Chen R. Size-Dependent Antibacterial Activities of Silver Nanoparticles against Oral Anaerobic Pathogenic Bacteria. J Mater Sci Mater Med. 2013. 24: 1465-1471.
38. Queitsch U, Mohn E, Schäffel F, Schultz L, Rellinghaus B, et al. Regular Arrangement of Nanoparticles from the Gas Phase on Bacterial Surface-Protein Layers. Appl Phys Lett. 2007. 90: 113114. CrossRef]
39. Brycki B, Koziróg A, Kowalczyk I, Pospieszny T, Materna P, et al. Synthesis Structure Surface and Antimicrobial Properties of New Oligomeric Quaternary Ammonium Salts with Aromatic Spacers. Molecules. 2017. 22: 1810.
40. Grueso E, Roldan E, Perez-Tejeda P, Kuliszewska E, Molero B, et al. Reversible DNA Compaction Induced by Partial Intercalation of 16-Ph-16 Gemini Surfactants: Evidence of Triple Helix Formation. Phys. Chem. Chem Phys. 2018. 20: 24902-24914.

Copyright: © 2025 Santhosh Kumar TN, et al. This is an open-access article distributed under the terms of the Creative Commons Attribution License, which permits unrestricted use, distribution, and reproduction in any medium, provided the original author and source are credited.